Structural and electronic properties of Bi-adsorbate-stabilized reconstructions on the InP(100) and $GaAs_xN_{1-x}(100)$ surfaces

P. Laukkanen, J. Pakarinen, M. Ahola-Tuomi, M. Kuzmin, R. E. Perälä, and I. J. Väyrynen
Department of Physics, University of Turku, FIN-20014 Turku, Finland

A. Tukiainen, J. Konttinen, P. Tuomisto, and M. Pessa
Optoelectronics Research Centre, Tampere University of Technology, FIN-33101 Tampere, Finland
(Received 12 June 2006; revised manuscript received 21 August 2006; published 4 October 2006)

Bismuth (Bi) adsorbate-stabilized reconstructions on the InP(100) and $GaAs_xN_{1-x}(100)$ surfaces have been studied by scanning tunneling microscopy (STM) and spectroscopy (STS), x-ray photoelectron spectroscopy, and low-energy electron diffraction. With decreasing coverage, Bi is found to stabilize the (2×1), (2×8), and (2×4) reconstructions on the InP(100) surface and the (2×1) and (2×4) reconstructions on the $GaAs_xN_{1-x}(100)$. STM results show that both the Bi/InP(100)(2×4) and Bi/$GaAs_xN_{1-x}(100)(2\times4)$ reconstructions can be described with the $\alpha2$-like structural model. The current-voltage curves measured by STS show the Bi/InP(100)(2×1) and Bi/$GaAs_xN_{1-x}(100)(2\times1)$ structures, which do not obey the electron counting model, to be semiconducting and metallic, respectively. Combining our experimental findings, we propose atomic models for the (2×1) reconstructions. An issue why Bi stabilizes unusual (2×1) structures is discussed.

DOI: 10.1103/PhysRevB.74.155302 PACS number(s): 68.35−p, 68.43.Hn, 73.61.Ey

I. INTRODUCTION

Various reconstructions of clean and adsorbate-stabilized III–V compound-semiconductor surfaces can be interpreted with the following driving mechanisms.[1] (i) Surface atoms dimerize to reduce the number of unsaturated dangling bonds. (ii) As the electron counting model (ECM) predicts,[2] dangling bonds of the electropositive atoms (group III) are empty and those of the electronegative atoms (group V) are doubly occupied, resulting in a semiconducting surface with vacant dimer sites. (iii) Spatial arrangement of dimers minimizes the electrostatic energy. However, some exceptional surfaces exist; for example, GaSb(100)$(n\times5)$ and Sb-stabilized GaAs(111)(1×3) reconstructions do not comply with the principle (ii).[3,4] Structural energies of these surfaces have been shown to be lowered enough to overcome the electronic energy cost associated with occupying the midgap or conduction-band states. Knowledge of the structural and electronic properties of such exceptional III-V surfaces is essential for a thorough understanding of physical mechanisms behind reconstructions.

Group-V adsorbate-stabilized III–V(100) surfaces such as Sb/GaAs(100) and As/InP(100) have attracted a lot of interest because they have an important role in the preparation (growth) of heteroepitaxial device structures (e.g., Refs. 5–10). Among these surface systems, the behavior of bismuth (Bi) on III–V(100) is less known. It has been shown very recently that on the GaAs(100) and InAs(100) surfaces, Bi stabilizes (2×4) reconstructions similar to the clean (i.e., As-stabilized) and Sb-stabilized GaAs(100)(2×4) and InAs(100)(2×4) reconstructions.[11,12] At the higher Bi coverage, the Bi/GaAs(100)(2×4) reconstruction is found to undergo a structural transition to an unusual (2×1) phase,[12] instead of the prototypical $c(4\times4)$ phase induced by As on the GaAs(100).[13] Such a small (2×1) unit cell necessarily violates the ECM concept,[2] and thus the Bi/GaAs(100)(2×1) surface can be expected to be metallic. Currently, it is, however, unclear whether the Bi/GaAs(100)(2×1) is metallic or semiconducting, and no atomic model has been proposed for this reconstruction. Interestingly, the (2×1) symmetry, which is characteristic for the Si(100) and Ge(100) surfaces, has been previously observed also on the P-stabilized InP(100) surface.[14] Furthermore, the P/InP(100)(2×1) surface has been found to be semiconducting, which has been proposed to be due to the electron-correlation effect.[14] Since then, it has been, however, shown that the InP(100)(2×1) reconstruction is not a clean surface but stabilized by hydrogen.[1,15]

Here, we report that Bi stabilizes unusual (2×1) reconstructions on the InP(100) and $GaAs_xN_{1-x}(100)$ surfaces, which have larger and smaller lattice constants than the GaAs(100) surface, respectively. The Bi/InP(100) and Bi/$GaAs_xN_{1-x}(100)$ surfaces have been studied by scanning tunneling microscopy (STM) and spectroscopy (STS), x-ray photoelectron spectroscopy (XPS), and low-energy electron diffraction (LEED). With decreasing coverage, bismuth is found to stabilize the (2×1), (2×8), and (2×4) reconstructions on the InP(100) surface and the (2×1) and (2×4) reconstructions on the $GaAs_xN_{1-x}(100)$ surface. Particularly, the properties of the Bi-stabilized (2×1) and (2×4) reconstructions have been investigated in this work. According to the STS results, the Bi/InP(100)(2×1) surface is semiconducting, and the Bi/$GaAs_xN_{1-x}(100)(2\times1)$ is metallic. Atomic models that explain the experimental results of the (2×1) and (2×4) reconstructions are proposed.

II. EXPERIMENTS

Measurements were performed in an Omicron ultrahigh-vacuum (UHV) system equipped with LEED, STM, and XPS. STM images were taken in the constant current mode,

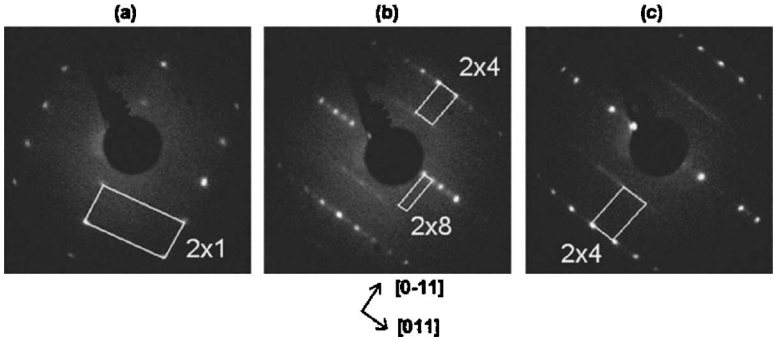

FIG. 1. (a) LEED (66 eV) from the Bi/InP(100)(2×1) surface heated to 340 °C, (b) LEED (79 eV) from the Bi/InP(100)(2×4)+(2×8) surface heated to 430 °C, and (c) LEED (48 eV) from the Bi/InP(100)(2×4) surface heated to 460 °C. The white rectangles represent the reciprocal unit cells.

and the tunneling spectroscopy was performed simultaneously with the topographic measurement. The Mg $K\alpha$ line (1253.6 eV) was used for excitation in XPS. All the measurements were carried out at room temperature (RT) in UHV with the pressure in the 10^{-11} mbar range.

The clean InP(100) substrates with the established mixed-dimer (2×4) surface structure were prepared according to the process described in Ref. 16. That is, the InP substrates were grown by molecular-beam epitaxy (MBE) on epiready *n*-type InP(100) wafers. The thermal desorption of native oxides was carried out at 515 °C for 10 min under a phosphorus flux, upon which the undoped InP layer with a thickness of 100 nm was grown at 490 °C. The substrate temperature was read with an infrared pyrometer. Indium was provided from a standard Knudsen effusion cell and phosphorus (P_2) from a three-zone valved cracker source.

Two different types of the capping layer were used in order to protect the grown InP(100) surfaces against air exposure during sample transfer between separate UHV systems. One cap was a double layer of phosphorus and arsenic: After the MBE growth, the substrate temperature was slowly reduced to near room temperature under the P_2 flux. After closing the P_2 source, the As_2 valve was opened and an amorphous arsenic layer was deposited on the surface for 35 min. Another cap was a pure phosphorus layer, which was deposited by keeping the grown surface at near room temperature under the P_2 flux for 30 min.

Both capping layers were removed by heating the InP(100) substrates to 420–450 °C in UHV. It repeatedly produced a clear 2×4 LEED pattern, which improved after heating the substrate up to 490 °C. According to STM observations, the double layer of phosphorus and arsenic protected the InP(100) surface better than the pure phosphorus layer since the observed clean mixed-dimer-reconstructed areas were larger on the former substrate. Thus, the substrate protected by the double layer of phosphorus and arsenic was used in this work. However, we tested the other substrate: STM observations showed that similar Bi-stabilized structures were obtained with the InP(100) substrate protected by the pure phosphorus cap.

A $GaAs_xN_{1-x}(100)$ substrate was grown on the GaAs(100) by MBE with a nitrogen plasma source. The nitrogen composition $1-x$ of the $GaAs_xN_{1-x}$ film was estimated to be 0.04. Upon the growth of 100-nm-thick $GaAs_xN_{1-x}$, the surface was protected against the air exposure by an arsenic capping layer deposited at RT. After the transfer through air, the protective layer was removed by heating the substrate in UHV up to 600 °C, which produced (4×2)-reconstructed $GaAs_xN_{1-x}(100)$ surface. A typical LEED pattern of this surface is shown in Fig. 2(c). Due to a limited sharpness of the 4×2 pattern, we cannot distinguish it from a $c(8\times2)$ pattern.

Approximately 1.5-monolayer (ML) thick Bi layers were evaporated from a W-coil source onto the InP(100)(2×4) and $GaAs_xN_{1-x}(100)(4\times2)$ surfaces held at RT. Then the Bi/InP(100) and Bi/$GaAs_xN_{1-x}(100)$ surfaces were heated gradually in UHV, as described below. Temperatures were measured by a pyrometer.

III. RESULTS AND DISCUSSION

Figures 1 and 2 show typical LEED patterns obtained from the Bi/InP(100) and Bi/$GaAs_xN_{1-x}(100)$ reconstructions, respectively, after heating the surfaces to different temperatures. The temperature ranges, in which different reconstructions were observed by LEED and STM, are summarized in Fig. 3. Also, the Bi 4*f* photoelectron intensities measured by XPS from the Bi/InP(100) and Bi/$GaAs_xN_{1-x}(100)$ reconstructions as a function of the heat-

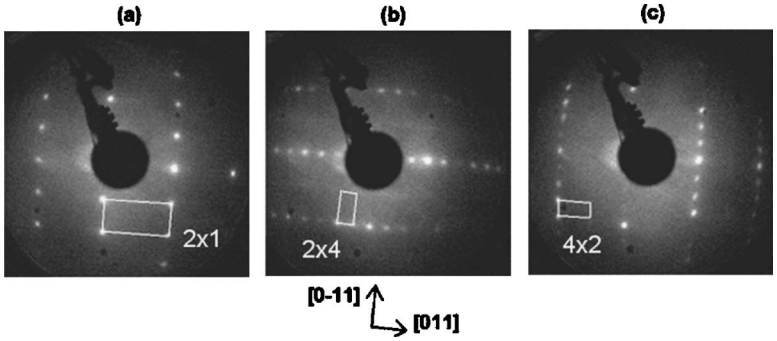

FIG. 2. (a) LEED (128 eV) from the Bi/$GaAs_xN_{1-x}(100)(2\times1)$ surface heated to 250 °C, (b) LEED (124 eV) from the Bi/$GaAs_xN_{1-x}(100)(2\times4)$ surface heated to 320 °C, and (c) LEED (123 eV) from the $GaAs_xN_{1-x}(100)(4\times2)$ surface heated to 580 °C. The white rectangles represent the reciprocal unit cells.

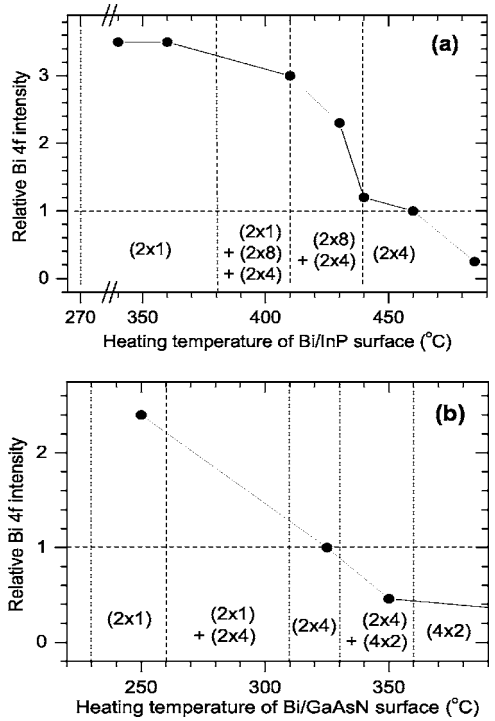

FIG. 3. The relative Bi $4f$ intensities (black dots represent data points) measured by XPS from the Bi/InP (a) and Bi/$GaAs_xN_{1-x}$ (b) surfaces as a function of the heating temperature. The vertical lines separate the temperature ranges where the different reconstructions were observed by LEED and STM.

ing temperature are presented in Fig. 3 in proportion to the intensities of the (2×4) reconstructions. From the Bi $4f$ measurements, we estimate that the Bi coverage of the Bi/InP(100)(2×1) surface is 3.5 times the coverage of the Bi/InP(100)(2×4) and that the corresponding coverage ratio between the Bi/$GaAs_xN_{1-x}$(100)(2×1) and (2×4) is 2.4. Moreover, the upper temperature limits for the Bi/InP(100) reconstructions are clearly higher than the corresponding ones for the Bi/$GaAs_xN_{1-x}$(100), as can be seen in Fig. 3, suggesting the Bi-induced reconstructions are thermally more stable on the InP(100) surface than on the $GaAs_xN_{1-x}$(100) surface.

Figure 4(a) presents a filled-state STM image of the Bi/InP(100)(2×4) surface that includes (2×8)-reconstructed areas [i.e., Bi/InP(100)$(2\times4)+(2\times8)$]. The Bi/InP(100)(2×8) reconstruction appears in Fig. 4(a) as white rows with a separation of about 33 Å. An atomic-resolution filled-state image of the (2×4)-reconstructed Bi/InP(100) surface is shown in Fig. 4(b). This image can well be explained with the $\alpha2$-like model having the Bi coverage of 0.5 ML [Fig. 4(c)]. The white paired maxima are related to the first-layer Bi-dimer atoms, and the rows of the gray maxima, located asymmetrically between the rows of the white features, are assigned to the third-layer Bi dimers. In passing, here we do not disentangle the (2×4) reconstruction from the $c(2\times8)$ one. The STM-line profiles (not shown) reveal a typical distance between two maxima of both the white and gray dimers to be about 3 Å, which is close to the double of a covalent radius of Bi atom (1.46 Å). However, based on our previous finding that in the Bi/InAs(100)(2×4)-$\alpha2$ reconstruction only half of the third-layer dimer sites are occupied by Bi atoms,[11] we propose the Bi coverage of the Bi/InP(100)(2×4) also to be 0.375 ML. In other words, half of the third-layer atoms of the Bi/InP(100)(2×4)-$\alpha2$ are proposed to be P ones. This is consistent with the fact that the starting mixed-dimer InP(100)(2×4) surface consists of 0.125 ML of P atoms, which can appear on the Bi/InP(100)(2×4) surface. Thus, we estimate, by means of the Bi $4f$ intensity ratio, the Bi coverage of the Bi/InP(100)(2×1) surface to be 1.3 ML.

It is worth noting that, in agreement with previous findings for the Bi/GaAs(100)(2×4) and Bi/InAs(100)(2×4) surfaces,[11,12] only the $\alpha2$-like structure was found on the Bi/InP(100)(2×4) surfaces heated to the different temperatures, covering the (2×4) and $(2\times4)+(2\times8)$ conditions in Fig. 3. That is, the behavior of the Bi/InP(100)(2×4) surface clearly differs from the clean InP(100)(2×4) reconstruction where the mixed-dimer phase dominates in a wide range of the preparation conditions and where the $\alpha2$ phase is stable only in a very limited range of the conditions.[16–21] The observation agrees with the theory showing the In-In dimer-related stress of the mixed-dimer structure to increase with a radius of the group-V atom.[19]

A clear difference between the Bi/InP and Bi/$GaAs_xN_{1-x}$(100)(2×4) surfaces is that the ordering of the white first-layer dimer rows is better on the former surface than on the latter one, as can be seen in the filled-state images of Figs. 4(b) and 5(a). This may arise from the different surface-lattice constants of $GaAs_xN_{1-x}$ (<4.0 Å) and InP (≈4.2 Å), leading to different interactions of the Bi dimers on these surfaces. For the Bi/$GaAs_xN_{1-x}$(100)(2×4) surface, the $\alpha2$-like structure is also proposed to be valid (Fig. 5). The white features of the empty-state STM image in Fig. 5(b) are related to the empty dangling bonds of

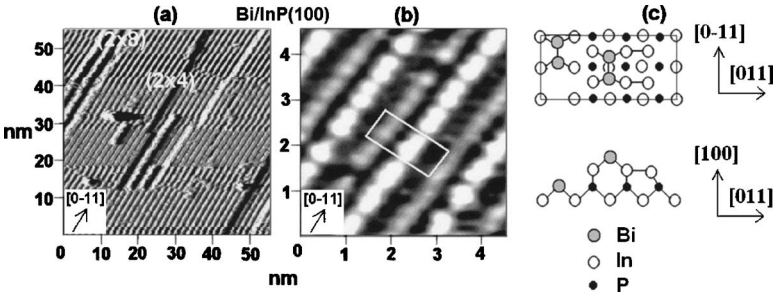

FIG. 4. (a) A filled-state STM image of the Bi/InP(100)(2×4) surface showing a local (2×8)-reconstructed area; the tunneling current is 0.46 nA and the voltage 2.15 V; the gray rectangle in the left top corner represents the (2×8) unit cell. (b) An atomic-resolution filled-state image of the Bi/InP(100)(2×4); the tunneling current is 0.42 nA and the voltage 1.80 V; the white rectangle represents the (2×4) unit cell. (c) The $\alpha2$-like unit-cell model proposed for the Bi/InP(100)(2×4).

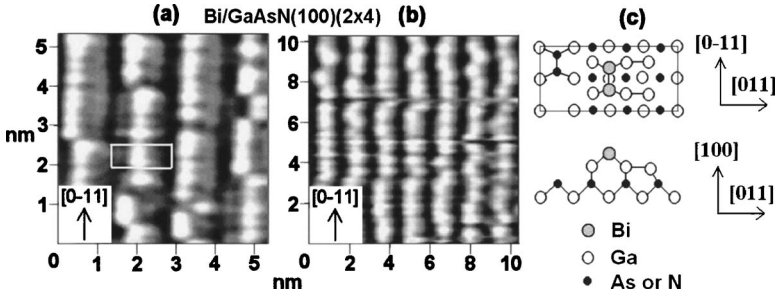

FIG. 5. (a) A filled-state STM image of the $Bi/GaAs_xN_{1-x}(100)(2\times4)$ surface; the tunneling current is 0.35 nA and the voltage 1.70 V; the white rectangle represents the unit cell. (b) An empty-state STM image of the $Bi/GaAs_xN_{1-x}(100)(2\times4)$ surface; the tunneling current is 0.21 nA and the voltage 1.70 V. (c) The $\alpha2$-like unit-cell model proposed for the $Bi/GaAs_xN_{1-x}(100)(2\times4)$.

the threefold-coordinated second-layer Ga atoms and/or of the first-layer mixed (Bi-Ga) dimer atoms[12] (not shown in the model of Fig. 5). Based on our previous observations that the Bi atoms lie only in the topmost atomic layer in the Bi/GaAs(100)(2×4)-$\alpha2$ reconstruction,[12] we propose the Bi coverage of the $Bi/GaAs_xN_{1-x}(100)(2\times4)$ surface similarly to be 0.25 ML. Thus, the coverage of the $Bi/GaAs_xN_{1-x}(100)(2\times1)$ reconstruction is approximately 0.6 ML, according to the Bi $4f$ intensity ratio.

Well-ordered (2×1)-reconstructed areas were found on both the Bi/InP(100) and $Bi/GaAs_xN_{1-x}(100)$ surfaces, as can be deduced from the LEED images (Figs. 1 and 2) and from the STM images of Figs. 6(a) and 6(d). Atomic resolution filled- and empty-state STM images of the Bi/InP(100)(2×1) are shown in Figs. 6(b) and 6(c), respectively. The protrusion *A* in Fig. 6(b) may arise from a filled or half-filled dangling bond of a dimer atom, while the protrusion *C* in Fig. 6(c) may be related to an empty or half-filled dangling bond. Some of the white filled-state protrusions, like *B*, are oblong in the [0–11] direction, indicating that the Bi/InP(100)(2×1) surface consists of two or more different unit cells. Similar interpretations apply to the filled- and empty-state features, *D* and *E*, in the STM images of the $Bi/GaAs_xN_{1-x}(100)(2\times1)$ surface in Figs. 6(e) and 6(f), respectively.

The current-voltage curve of the $Bi/GaAs_xN_{1-x}(100)\times(2\times1)$ in Fig. 7 shows this surface to be metallic, as can be expected on the basis of the ECM concept. In contrast, the Bi/InP(100)(2×1) surface surprisingly appears to be semiconducting. The curve of the $Bi/GaAs_xN_{1-x}(100)(2\times4)$ surface, which obeys the ECM and is semiconducting, is presented in Fig. 7 for comparison. The inset shows the differential curves, which are proportional to the electronic density of states.[22] Figure 7 shows that the surface band gaps are approximately 0.8 and 1.4 eV for the Bi/InP(100)(2×1) and $Bi/GaAs_xN_{1-x}(100)(2\times4)$, respectively. The band gap of the Bi/InP(100)(2×1) surface is smaller than 1.2 ± 0.2 eV found previously on the P/InP(100)(2×1) surface.[14] Nowadays, it is accepted that the P/InP(100)$\times(2\times1)$ surface is terminated by hydrogen,[1,15] as mentioned in Sec. I. Here, such bonding of hydrogen to Bi dimers (i.e., one H atom per dimer) is, however, unlikely due to the surface-preparation conditions.

Combining the observations, we propose in Fig. 8 tentative atomic models for the (2×1) reconstructions. The Bi coverages for the models in Figs. 8(a) and 8(b) are 1 and 0.5 ML, respectively. Since the coverage of the $Bi/GaAs_xN_{1-x}(100)(2\times1)$ surface was estimated to be 0.6 ML, we suggest the structure in Fig. 8(b) dominates on the $Bi/GaAs_xN_{1-x}(100)(2\times1)$ surface and that the structure of Fig. 8(a) appears only locally. Both of the models violate the ECM because not all dangling bonds of the Bi atoms can be doubly occupied, agreeing with the metallic character of the $Bi/GaAs_xN_{1-x}(100)(2\times1)$ surface. Furthermore, the filled-state STM protrusion *D* of the $Bi/GaAs_xN_{1-x}(100)(2\times1)$ in Fig. 6(e) is related to a half-filled Bi dangling bond of the mixed In-Bi dimer, whereas the empty-state protrusion *E* in

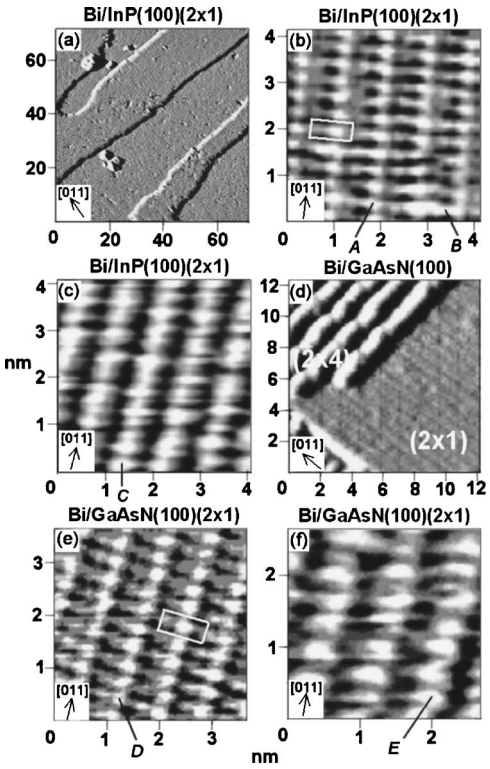

FIG. 6. (a) A large-scale filled-state STM image of the Bi/InP(100)(2×1) surface; the tunneling current is 3.34 nA and the voltage 2.63 V. (b) An atomic-resolution filled-state image of the Bi/InP(100)(2×1) surface; the tunneling current is 0.51 nA and the voltage 1.73 V; the white rectangle represents the unit cell. (c) An empty-state image of the Bi/InP(100)(2×1); the tunneling current is 3.87 nA and the voltage 1.00 V. (d) A filled-state STM image of the $Bi/GaAs_xN_{1-x}(100)(2\times1)+(2\times4)$ surface; the tunneling current is 0.42 nA and the voltage 2.94 V. (e) An atomic-resolution filled-state STM image of the $Bi/GaAs_xN_{1-x}(100)(2\times1)$; the tunneling current is 0.51 nA and the voltage 1.39 V; the white rectangle represents the unit cell. (f) An empty-state STM image of the $Bi/GaAs_xN_{1-x}(100)(2\times1)$; the tunneling current is 0.25 nA and the voltage 1.55 V.

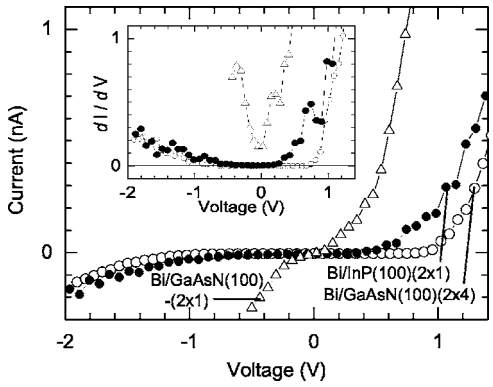

FIG. 7. The current-voltage curves, $I(V)$, measured from the Bi/InP(100)(2×1), Bi/GaAs$_x$N$_{1-x}$(100)(2×1), and Bi/GaAs$_x$N$_{1-x}$(100)(2×4) surfaces using STS. The tunneling spectroscopy was performed simultaneously with the topographic measurement using the filled-state voltage of 3.56 V and the current of 0.97 nA for the Bi/InP surface and the filled-state voltage of 3.04 V and the current of 0.50 nA for the Bi/GaAs$_x$N$_{1-x}$ surfaces. The inset shows the corresponding differential curves, $dI/dV(V)$, which are proportional to the electronic density of states.

Fig. 6(f) is proposed to arise from an empty In dangling bond and/or a half-filled Bi dangling bond of the mixed In-Bi dimer.

Since the Bi coverage of the Bi/InP(100)(2×1) was estimated to be 1.3 ML, the model in Fig. 8(a) is more plausible for this surface than the model of Fig. 8(b). The discrepancy in the coverage can be due to a replacement of the second-layer In atoms by Bi in the actual Bi/InP(100)(2×1) structure, which is not shown in the model of Fig. 8. Such Bi antisites can also make the Bi/InP(100)(2×1) structure more stable than the Bi/GaAs$_x$N$_{1-x}$(100)(2×1) via the formation of strong group-V-group-V bonds,[4] agreeing with the finding that higher temperatures were needed to remove the Bi-stabilized (2×1) reconstruction from the InP(100) than GaAs$_x$N$_{1-x}$(100) surface and that the Bi/InP(100)(2×1) reconstruction was stable in a wide temperature range (Fig. 3). Another reason for this coverage discrepancy can simply be an erroneous determination of the Bi amount of the Bi/InP(100)(2×1). For example, defects like Bi clusters on the Bi/InP(100)(2×1) surface can cause such overestimation of the coverage from the Bi $4f$ intensity-ratio measurements.

The filled-state STM protrusion A of the Bi/InP(100)(2×1) in Fig. 6(b) is interpreted to arise from a doubly occupied dangling bond of the Bi-Bi dimer, and the empty-state protrusion C in Fig. 6(c) is related to a half-filled Bi dangling bond. Furthermore, the semiconducting character of the Bi/InP(100)(2×1) surface is suggested to be due to the electron-correlation effect or inequivalent dimers,[14,23] however future investigations are required to clarify the observed energy gap of the Bi/InP(100)(2×1) surface.

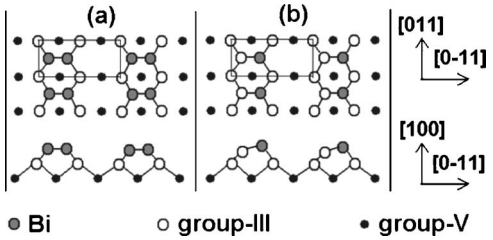

FIG. 8. Atomic models proposed for the Bi-stabilized (2×1) reconstructions. For details, see the text.

Several III–V(100) surfaces, e.g., P/InP(100)$c(4\times4)$,[24] obey the ECM and have dimer vacancies. Thus, an interesting question is why the Bi/InP and Bi/GaAs$_x$N$_{1-x}$(100)$\times(2\times1)$ surfaces without dimer vacancies are stable. One reason may be that the surface stress, related to dimers,[25,26] is considerably reduced on these (2×1) surfaces. The longer bond lengths of the Bi dimers, as compared to the P and As dimers, can lead to a reduced surface stress, which is in a balance with the continuous dimer rows,[4] making the formation of the Bi-induced (2×1) reconstructions possible. However, the electronic energy cost of a metallic surface structure does not appear to be compensable for the Bi/InP(100)(2×1) system, in contrast to the Bi/GaAs$_x$N$_{1-x}$(100)(2×1) surface where the surface-stress relief seems to overcompensate the electronic energy cost. This may be related to the smaller lattice constant of the GaAs$_x$N$_{1-x}$(100) surface as compared to the InP(100) one; that is, the Bi-Bi dimers ($\approx$3 Å in length) may accommodate better on the GaAs$_x$N$_{1-x}$(100) surface than on the InP(100) surface.

IV. CONCLUSIONS

With decreasing coverage, Bi is found to stabilize the (2×1), (2×8), and (2×4) reconstructions on the InP(100) and the (2×1) and (2×4) reconstructions on the GaAs$_x$N$_{1-x}$(100) surface. The $\alpha2$-like structural model explains the STM observations of both the Bi/InP(100)(2×4) and Bi/GaAs$_x$N$_{1-x}$(100)(2×4) surfaces. The current-voltage properties measured by STS show the Bi/InP(100)$\times(2\times1)$ and Bi/GaAs$_x$N$_{1-x}$(100)(2×1) surfaces to be semiconducting and metallic, respectively. On the basis of the experimental findings, atomic models are proposed for the (2×1) reconstructions, and the differences of these surfaces are tentatively discussed. Theoretical calculations and complementary measurements are needed to establish the models and to solve the question why Bi stabilizes the unusual (2×1) reconstructions.

ACKNOWLEDGMENTS

We thank W. G. Schmidt for valuable discussions and H. Ollila for technical assistance. This work has been supported in part by the Academy of Finland Grant No. 205766 (I.J.V.) and by TEKES within Project No. 40126/05.

[1] W. G. Schmidt, P. H. Hahn, F. Bechstedt, N. Esser, P. Vogt, A. Wange, and W. Richter, Phys. Rev. Lett. **90**, 126101 (2003).
[2] M. D. Pashley, Phys. Rev. B **40**, 10481 (1989).
[3] P. Moriarty, P. H. Beton, M. Henini, and D. A. Woolf, Surf. Sci. **365**, L663 (1996).
[4] L. J. Whitman, P. M. Thibado, S. C. Erwin, B. R. Bennett, and B. V. Shanabrook, Phys. Rev. Lett. **79**, 693 (1997).
[5] B. Z. Nosho, W. H. Weinberg, W. Barvosa-Carter, B. R. Bennett, B. V. Shanabrook, and L. J. Whitman, Appl. Phys. Lett. **74**, 1704 (1999).
[6] F. Maeda, Y. Watanabe, and M. Oshima, Phys. Rev. B **48**, R14733 (1993).
[7] P. Moriarty, P. H. Beton, Y.-R. Ma, M. Henini, and D. A. Woolf, Phys. Rev. B **53**, R16148 (1996).
[8] N. Esser, A. I. Shkrebtii, U. Resch-Esser, C. Springer, W. Richter, W. G. Schmidt, F. Bechstedt, and R. Del Sole, Phys. Rev. Lett. **77**, 4402 (1996).
[9] Q.-K. Xue, T. Hashizume, and T. Sakurai, Prog. Surf. Sci. **56**, 1 (1997).
[10] C. H. Li, L. Li, D. C. Law, S. B. Visbeck, and R. F. Hicks, Phys. Rev. B **65**, 205322 (2002).
[11] P. Laukkanen, M. Ahola, M. Kuzmin, R. E. Perälä, I. J. Väyrynen, and J. Sadowski, Surf. Sci. **598**, L361 (2005).
[12] M. Ahola-Tuomi, P. Laukkanen, R. E. Perälä, M. Kuzmin, J. Pakarinen, I. J. Väyrynen, and M. Adell, Surf. Sci. **600**, 2349 (2006).
[13] A. Ohtake, J. Nakamura, S. Tsukamoto, N. Koguchi, and A. Natori, Phys. Rev. Lett. **89**, 206102 (2002).
[14] L. Li, B.-K. Han, Q. Fu, and R. F. Hicks, Phys. Rev. Lett. **82**, 1879 (1999).
[15] G. Chen, S. F. Cheng, D. J. Tobin, L. Li, K. Raghavachari, and R. F. Hicks, Phys. Rev. B **68**, 121303(R) (2003).
[16] P. Laukkanen, J. Pakarinen, M. Ahola-Tuomi, M. Kuzmin, R. E. Perälä, I. J. Väyrynen, A. Tukiainen, V. Rimpiläinen, M. Pessa, M. Adell, and J. Sadowski, Surf. Sci. **600**, 3022 (2006).
[17] C. D. MacPherson, R. A. Wolkow, C. E. J. Mitchell, and A. B. McLean, Phys. Rev. Lett. **77**, 691 (1996).
[18] W. G. Schmidt, F. Bechstedt, N. Esser, M. Pristovsek, Ch. Schultz, and W. Richter, Phys. Rev. B **57**, 14596 (1998).
[19] S. Mirbt, N. Moll, K. Cho, and J. D. Joannopoulos, Phys. Rev. B **60**, 13283 (1999).
[20] N. Esser, W. G. Schmidt, J. Bernholc, A. M. Frisch, P. Vogt, M. Zorn, M. Pristovsek, W. Richter, F. Bechstedt, Th. Hannappel, and S. Visbeck, J. Vac. Sci. Technol. B **17**, 1691 (1999).
[21] L. Li, Q. Fu, C. H. Li, B.-K. Han, and R. F. Hicks, Phys. Rev. B **61**, 10223 (2000).
[22] R. M. Feenstra, Phys. Rev. B **50**, 4561 (1994).
[23] W. G. Schmidt, Appl. Phys. A **75**, 89 (2002).
[24] V. P. LaBella, Z. Ding, D. W. Bullock, C. Emery, and P. M. Thibado, J. Vac. Sci. Technol. A **18**, 1492 (2000).
[25] O. L. Alerhand, A. N. Berker, J. D. Joannopoulos, D. Vanderbilt, R. J. Hamers, and J. E. Demuth, Phys. Rev. Lett. **64**, 2406 (1990).
[26] J. Tersoff, Phys. Rev. B **45**, 8833 (1992).